

Guided Filtering using Reflected IR Image for Improving Quality of Depth Image

Takahiro Hasegawa, Ryoji Tomizawa, Yuji Yamauchi, Takayoshi Yamashita and Hironobu Fujiyoshi
Chubu University, 1200, Matsumoto-cho, Kasugai, Aichi, Japan

Keywords: Guided Filter, Reflected IR Image, Depth Image, Denoising, Upsampling.

Abstract: We propose the use of a reflected IR image as a guide image to improve the quality of depth image. Guided filtering is a technique that can quickly remove noise from a depth image by using a guide image. However, when an RGB image is used as a guide image, the quality of depth image does not be improved if the RGB image contains texture information (such as surface patterns and shadows). In this study, our aim is to obtain a depth image of higher quality by using a guide image derived from a reflected IR image, which have less texture information and a high correlation with depth image. Using reflected IR image, it is possible to perform filtering while retaining edge information between objects of different materials, without being affected by textures on the surfaces of these objects. In evaluation experiments, we confirmed that a guide image based on reflected IR image produce better denoising effects than RGB guide image. From the results of upsampling tests, we also confirmed that the proposed IR based guided filtering has a higher PSNR than that of RGB image.

1 INTRODUCTION

Time-of-flight (TOF) cameras (Lange and Seitz, 2001) are widely used in computer vision as sensors for the acquisition of depth information (May et al., 2006) (Fang et al., 2009). In particular, Kinect cameras have been used to estimate human poses from a depth image as a gesture input for computer games (Shotton et al., 2011). A TOF camera measures the distance to an object by using phase differences to determine the time it takes for infrared light from an LED to be reflected back to the camera from an object (Hansard et al., 2013) (Foix et al., 2011). However, depth image from a TOF camera is susceptible to noise from external light disturbance due to the fact that the energy of infrared photons decreases as their time of flight increases. Since a noisy depth image can lead to impaired object recognition and object detection performance (Ikemura and Fujiyoshi, 2012), pre-processing measures such as noise removal are necessary. Also, a depth image is generally of low resolution due to hardware constraints on camera sensors (Kolb et al., 2009), but a higher resolution image is needed in many applications.

Noise elimination and upsampling from depth image are achieved by Gaussian filter, bilateral filter (Tomasi, 1998), non-local means filter (Buades et al., 2005) and guided filter (Kaiming et al., 2013). Al-

though a Gaussian filter reduces noise, it also smooths out the required edges between objects. A joint bilateral filter (Petschnigg et al., 2004) (Eisemann and Durand, 2004) is an enhanced form of bilateral filter that uses two types of image a noisy input image and a reference image with reduced noise to remove noise from the input image by filtering determined based on the pixel values of the reference image. A bilateral filter and a joint bilateral filter are used to upsample the depth image (Yang et al., 2007) (Kopf et al., 2007). While a bilateral filter and joint bilateral filter are capable of smoothing out images while preserving edges, its high computational cost results in problems due to slow processing times. A non-local means filter (Buades et al., 2005) creates a local region for each pixel of an image as a template. It also defines a support window that is wider than the template region. The weights of the support window are decided by similarity of template matching. A non-local means filter effectively removes noise from the image by convoluting it with support windows calculated for each pixel. Furthermore, a non-local means filter is used for upsampling of depth images (Park et al., 2011). However, it has a high computational cost because the support window is calculated for each pixel. A guided filter (Kaiming et al., 2013) is a filter that removes noise by using an im-

age captured in the same scene as the input image. A guided filter uses edge information from a guide image, which enables it to preserve edges in the depth image. It also has a low computational cost, and can thus be processed at high speed. Furthermore, given a high-resolution guide image, it can also upsample a low-resolution input image by interpolation. However, when an RGB image is used as the guide image, the depth image can become degraded due to texture information (object patterns, shadows, etc.) that is not present in the depth image.

In this paper we propose enhancing a depth image by guided filter using a reflected infrared (IR) image. A reflected IR image is obtained by intensity value which reflected infrared light from an object. A reflected IR image has no unnecessary texture information and is strongly correlated with the depth image, because it uses reflection of infrared light as with depth image. Therefore, the proposed method produces a high-quality depth image that is unaffected by texture information by using reflected IR image. The remainder of the paper is organized as follows. Section 2 discusses conventional guided filtering. Section 3 introduces the proposed method. Section 4 presents the experimental results, and the paper is concluded in the section 5.

2 GUIDED FILTER

This section discusses the guided filtering process, and the denoising and upsampling performed using a guided filter.

2.1 Guided Filtering Process

A guided filter is an edge-preserving noise removal filter that filters a depth image by using a guide image captured in the same scene as the target depth image. This is based on the idea that the output image of a guided filter is represented by a linear transform of the guide image. The processing flow of a guided filter is shown in Figure 1. In a local region ω_k , the coefficients (a_k, b_k) used for linear transformation are optimized so as to minimize the following cost function E :

$$E(a_k, b_k) = \frac{1}{|\omega_k|} \sum_i ((a_k I_i + b_k - p_i)^2 + \epsilon a_k^2), \quad (1)$$

where ϵ is a smoothing coefficient, ω is the local region, I_i represents the pixel values of the guide image, and p_i represents the pixel values of the input image. The resulting coefficients (a_k, b_k) are used to

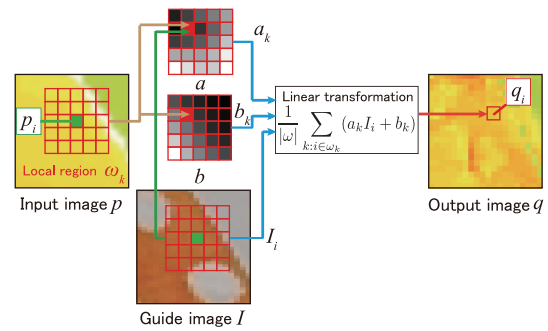


Figure 1: Guided filter processing.

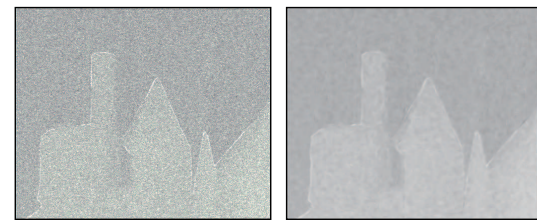


Figure 2: Denoising with a guided filter.

estimate the output image pixels q_i according to the linear transform of Equation (2):

$$q_i = \frac{1}{|\omega|} \sum_{k:i \in \omega_k} (a_k I_i + b_k). \quad (2)$$

2.2 The Issues of Guided Filtering

The guided filtering is used for denoising and up sampling. Like a bilateral filter, a guided filter is able to remove noise while preserving edges. In a bilateral filter, noise is removed by using information from the input image alone. But in a guided filter, it is possible to remove noise more efficiently by adding the information of a noiseless guide image. Figure 2 shows an example of denoising applied to a noisy depth image. A guided filter makes it possible to perform upsampling using a guide image of higher resolution than the input image. For a low-resolution input image, all the pixel coefficients (a_k, b_k) from the guide image are calculated, and for pixels that do not have the signal components of the input image, the pixel values are calculated according to Equation (2). In this way, it is possible to perform upsampling by interpolating from a low-resolution image. Figure 3 shows an example where a 320×240 pixel depth image is upsampled to 640×480 pixels by using a guided filter.

Although a guided filter can perform edge-preserving filter processing, problems can arise when a RGB image is used as the guide image due to the effects of textures that are not present in the depth image, as shown in Figure 4. This is because filtering is

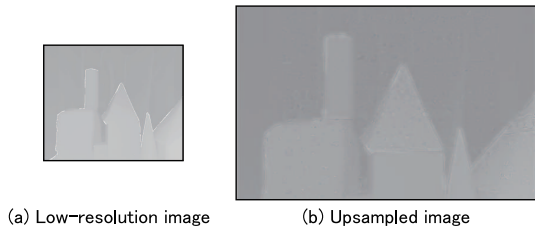


Figure 3: Upsampling with a guided filter.

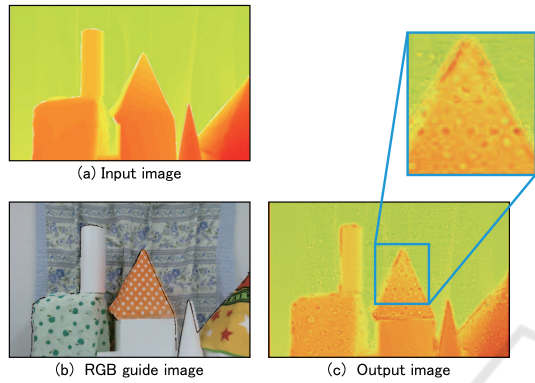


Figure 4: Result of guided filtering using an RGB guide image.

performed using texture information that is not originally present in the depth image.

3 GUIDED FILTERING USING A REFLECTED IR IMAGE

In this study, we use a reflected IR image obtained from TOF camera which is used for computing depth information, in order to prevent the depth image from being spoiled by the effects of unwanted texture information. This section examines the characteristics of infrared light and discusses the proposed method of using a reflected IR image.

3.1 Characteristics of Reflected Infrared Light

Intensity of IR reflection varies according to the distance to the object, the orientation of the reflecting surfaces, and the object's material. In this section, we examine the characteristics of reflected IR.

3.1.1 Characteristics of Change with Depth

The pixel values of the reflected IR image are the reflection values of infrared light, which vary with the object's depth from the camera. Figure 5 shows how the reflected IR values vary with depth. According to

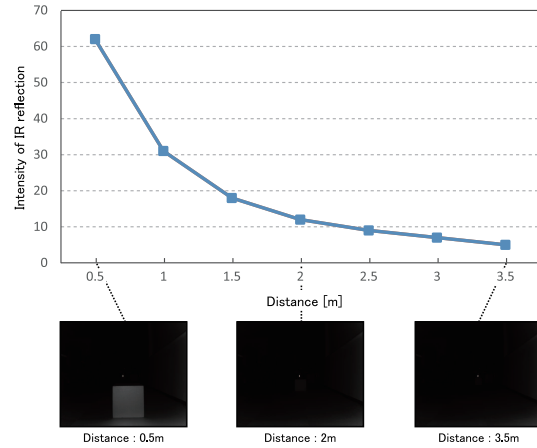


Figure 5: Variation of reflection intensity with depth.

Figure 5, at depths of over 2 m, the reflected IR values become so small that objects cannot be distinguished in the resulting image. If this is used as a guide image, then pixels captured from objects distant from the camera will be of no use for filtering.

3.1.2 Characteristics of Reflecting Surface Orientation

When the orientation of the reflecting surface of the object changes, the amount of light reflected also changes significantly. Figure 6 shows how the reflected IR changes with the angle of the reflecting surface of objects placed at equal depths. From Figure 6, it can be seen that as the angle of the reflecting surface increases, the reflected IR is attenuated. If this is used as a guide image, then no filtering effect will be obtained in pixels where the reflecting surface has a large angle.

3.1.3 Characteristics of the Material

The reflection of light varies according to the reflection characteristics of the object's material. Figure 7 shows the different IR reflection intensities of materials placed at the same distance with their reflecting surfaces at an angle of 0° . From this figure, it can be seen that the reflected IR varies with the object's material. However, since estimating materials is generally a difficult problem, in this study we do not consider changes of material.

3.2 Using Reflected IR Image

By performing guided filtering using a reflected IR image, we can obtain a high-quality depth image. A reflected IR image is suitable as a guide image for guided filtering because it has no textures or patterns

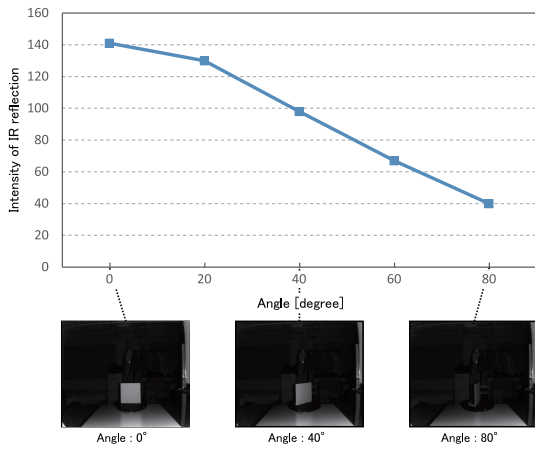


Figure 6: Variation of reflection intensity with the angle of the reflecting surface.

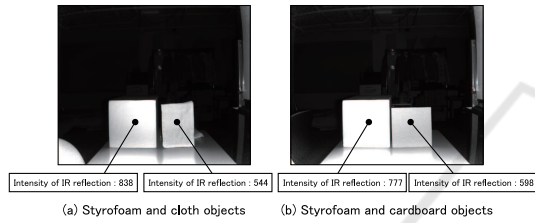


Figure 7: Variation of reflected IR with material.

that are included in an RGB image, and is strongly correlated with the depth image. However, since a reflected IR image has the characteristics shown in subsection 3.1, it is not possible to use the raw data directly as a guide image. Therefore, the reflected IR image is normalized to take these characteristics into account. The illuminance E of light L from the light source at the object surface is known to attenuate according to the depth d of the object and the angle θ of the light, as shown in Figure 8.

$$E = \frac{L}{(2 * d)^2} \cos \theta \quad (3)$$

In this study, the reflected IR image is normalized using the object's depth and the angle of the reflecting surface.

3.2.1 Normalization According to Depth

Since the infrared light from a TOF camera attenuates with increasing depth as shown in Equation (3), the reflected IR decreases. Therefore, the depth data is used to normalize the reflected IR image according to Equation (4):

$$G(i, j) = I(i, j) * (2 * d(i, j))^2, \quad (4)$$

where $d(i, j)$ is the distance value at coordinates (i, j) , and G is the reflected IR image after normalization.

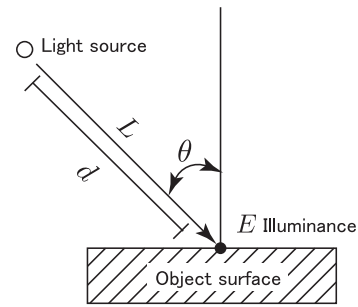


Figure 8: Attenuation of light according to the object depth and light angle.

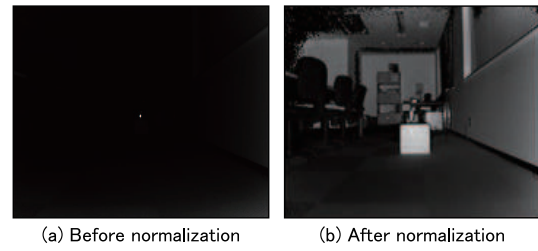


Figure 9: Normalization according to depth.

Since light is attenuated in proportion to the square of the depth, we can use Equation (4) to restore the reflected IR values. Figure 9 shows an example of a reflected IR image normalized using Equation (4).

3.2.2 Normalization According to Depth and Reflecting Surface Orientation

The intensity values of the reflected IR image vary according to the orientation of the reflecting surfaces of the objects. Therefore, the reflected IR image is normalized using the reflecting surface orientation calculated from the depth image. From Equation (3), normalization according to the orientation of the reflecting surfaces at the angle of coordinate (i, j) is performed as shown in Equation (5). Guided filtering is then performed using the reflected IR image normalized in this way as a guide image.

$$G(i, j) = \frac{I(i, j) * (2 * d(i, j))^2}{\cos \theta_x * \cos \theta_y} \quad (5)$$

$$\theta_x(i, j) = \tan^{-1} \frac{d(i+1, j) - d(i-1, j)}{(i+1) - (i-1)} \quad (6)$$

$$\theta_y(i, j) = \tan^{-1} \frac{d(i, j+1) - d(i, j-1)}{(j+1) - (j-1)} \quad (7)$$

θ_x and θ_y are the angles of the reflecting surface in the x and y directions as estimated from the neighboring pixels in the reflected IR image. According to Equation (5), the image is simultaneously normalized based on the camera-to-object depth $d(i, j)$ and the reflecting surface orientation θ_x and θ_y . Figure

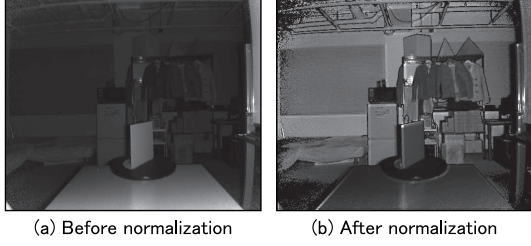


Figure 10: Normalization according to depth and reflecting surface orientation.

10 shows an example of a reflected IR image where the depth and reflecting surface orientations have been normalized simultaneously. By performing normalization according to the orientation of reflecting surfaces, it is possible to suppress the attenuation of reflected IR according to the orientation of the subject surfaces.

4 EXPERIMENTAL RESULTS

We performed evaluation tests to demonstrate the effectiveness of guided filtering using a reflected IR image. These tests were focused on denoising and upsampling.

4.1 Experimental Overview

In this experiments, we compared the proposed method (IR guide) with a conventional method (RGB guide) using a guide filter with an RGB image as the guide. The evaluation was performed using the peak signal-to-noise ratio (PSNR) obtained from the following equation:

$$PSNR = 20 \log_{10} \left(\frac{MAX}{\sqrt{MSE}} \right) [dB], \quad (8)$$

$$MSE = \frac{1}{mn} \sum_{i=0}^{m-1} \sum_{j=0}^{n-1} (X(i, j) - X'(i, j))^2, \quad (9)$$

where MAX is the maximum value that can be obtained among the true pixel values ($m \times n$ pixels), and MSE is the mean square error between the original pixels X and the filtered pixels X' . For the true values, we used the output of a 5×5 median filter applied to the depth image. The images used in the tests consisted of 178 images of the structure shown in Figure 11 with various different textures. The images were all 512×424 pixels in size.

In the denoising tests, Gaussian noise (mean = 0, $\sigma = 0.02$) was added to the depth image in order to confirm the noise removal effects. In the upsampling tests, the depth images were reduced to one quarter of their original size simply by decimating pixels.

We then evaluated the results of upsampling these reduced images.

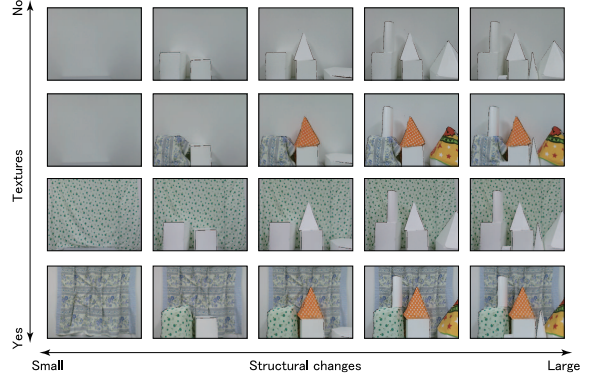


Figure 11: Evaluation data set.

4.2 Evaluation of Denoising Effects

Table 1 shows the PSNR of each method in the denoising tests. From Table 1, it can be confirmed that the PSNR values of the normalized reflected IR image are larger than those of images obtained using RGB guide images or median filtering. The reflected IR images obtained by normalizing both for depth and orientation of reflecting surfaces resulted in PSNR values that were slightly lower than those obtained with reflected IR images normalized for depth alone. This is because that noise added to the depth image causes instability in the estimation of the reflecting surface angles θ_x and θ_y . Figure 12 shows an example of a guided filter being used to remove noise from a depth image with added noise. From Fig. 12, it can be confirmed that an IR guide image was better than an RGB guide image for removing noise while suppressing the effects of textures on the object surface.

4.3 Evaluation of Upsampling Effects

Table 2 shows the PSNR of each method in upsampling. Like with denoising, it can be seen that the normalized reflected IR image resulted in higher PSNR values than the conventional RGB image. Also, the reflected IR images obtained by normalizing both for depth and orientation of reflecting surfaces resulted in PSNR values that were equal to or higher than those obtained with reflected IR images normalized for depth alone. This is thought to be because when the effects of noise on the input image were small, the angles θ_x and θ_y of the object's reflecting surface were estimated stably so that the PSNR was increased by including normalization according to the reflecting surface orientation.

Figure 13 shows examples of low-resolution

Table 1: PSNR of each method in denoising [dB].

Texture	Structural changes	Median filter	Guided image			
			RGB image	reflected IR image		
				Without normalization	Depth	Depth + orientation
No	Small	30.85	32.76	23.43	34.92	34.86
Yes	Small	30.57	32.51	23.37	34.91	34.78
No	Large	30.29	32.22	23.26	34.27	34.19
Yes	Large	30.14	31.96	23.19	34.23	34.17

Table 2: PSNR of each method in upsampling [dB].

Texture	Structural changes	RGB image	Guided image		
			reflected IR image		
			Without normalization	Depth	Depth + orientation
No	Small	19.76	8.43	20.64	20.67
Yes	Small	19.62	8.37	20.60	20.62
No	Large	19.48	8.26	20.18	20.23
Yes	Large	19.27	8.19	20.18	20.16

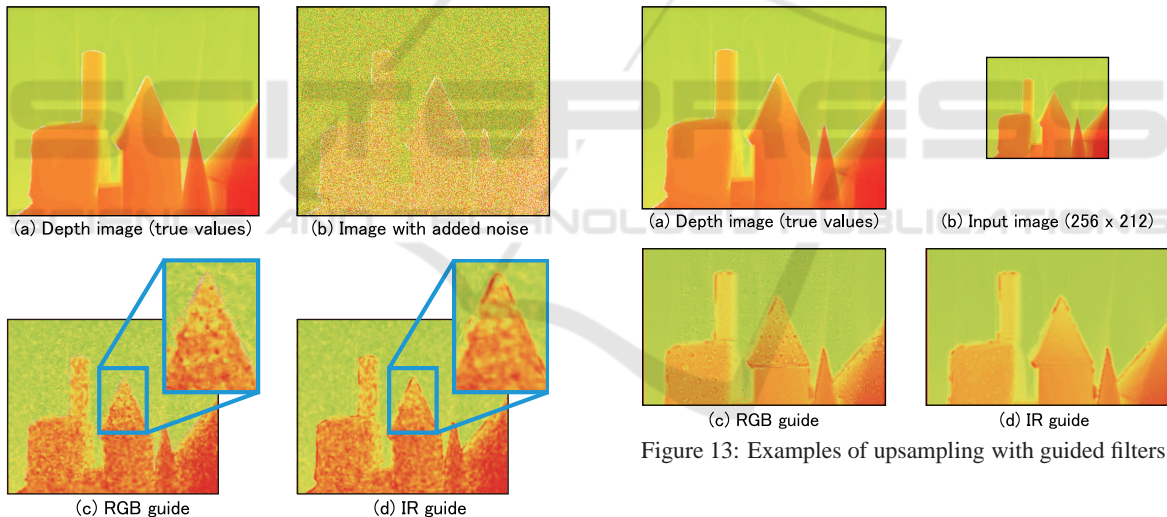


Figure 12: Examples of noise elimination with guided filters.

depth images upsampled by guided filters. From Fig. 13, it can be seen that it was possible to restore a 1/4 size image to its original size. When using an RGB guide image, the object's surface texture is left behind in the upsampled image, but with a reflected IR image, it can be seen that the depth image is almost completely unaffected by texture.

5 CONCLUSIONS

We have produced a depth image of higher quality by introducing the use of reflected IR image in guided filters. We have confirmed that a greater denoising effect can be achieved by normalizing a reflected IR image according to the depth of objects than by guided filtering using a conventional RGB image as the guide. Also, when a depth image with low noise is upsampled, we confirmed that it is possible to achieve higher quality upsampling by using a reflected IR image that has been normalized by depth and by the orientation of the reflecting surfaces. In the future works, we confirm effectiveness of the pro-

posed method by comparing other filtering algorithms such as non-local means filter (Buades et al., 2005) and bilateral filter (Tomasi, 1998). Also, we will study how to exploit the benefits of each type of image to achieve higher quality by combining an RGB image and a reflected IR image.

REFERENCES

- Buades, A., Coll, B., and Morel, J. M. (2005). A Non-Local Algorithm for Image Denoising. In *Conference on Computer Vision and Pattern Recognition*, pages 60–65.
- Eisemann, E. and Durand, F. (2004). Flash Photography Enhancement via Intrinsic Relighting. *ACM Transactions on Graphics*, 23(3):673–678.
- Fang, Y., Swadzba, A., Philippsen, R., Engin, O., Hanheide, M., and Wachsmuth, S. (2009). Laser-based navigation enhanced with 3d time-of-flight data. In *Robotics and Automation, 2009. ICRA '09. IEEE International Conference on*, pages 2844–2850.
- Foix, S., Alenya, G., and Torras, C. (2011). Lock-in Time-of-Flight (ToF) Cameras: A Survey. *IEEE Sensors Journal*, 11(9):1917–1926.
- Hansard, M., Lee, S., Choi, O., and Horaud, R. (2013). *Time-of-Flight Cameras - Principles, Methods and Applications*. Springer Briefs in Computer Science. Springer.
- Ikemura, S. and Fujiyoshi, H. (2012). No Title Human Detection by Haar-like Filtering using Depth Information. In *International Conference on Pattern Recognition*, pages 813–816.
- Kaiming, H., Jian, S., and Xiaoou, T. (2013). Guided Image Filtering. *IEEE Transactions on Pattern Analysis and Machine Intelligence*, 35(6):1397–1409.
- Kolb, A., Barth, E., Koch, R., and Larsen, R. (2009). Time-of-Flight Cameras in Computer Graphics. *Computer Graphics Forum*.
- Kopf, J., Cohen, M. F., Lischinski, D., and Uyttendaele, M. (2007). Joint Bilateral Upsampling. *ACM Transactions on Graphics*, 26(3).
- Lange, R. and Seitz, P. (2001). Solid-State Time-of-Flight Range Camera. *IEEE Journal of Quantum Electronics*, 37(3):390–397.
- May, S., Werner, B., Surmann, H., and Pervolz, K. (2006). 3D time-of-flight cameras for mobile robotics. In *International Conference on Intelligent Robots and Systems*, pages 790–795.
- Park, J., Kim, H., Tai, Y.-W., Brown, M., and Kweon, I. (2011). High Quality Depth Map Upsampling for 3D-TOF Cameras. In *International Conference of Computer Vision*.
- Petschnigg, J., Szeliski, R., Agrawala, M., Cohen, M., Hoppe, H., and Toyama, K. (2004). Digital photography with flash and no-flash image pairs. *ACM Transactions on Graphics*, 23(3):664–672.
- Shotton, J., Fitzgibbon, A., Cook, M., Sharp, T., Finocchio, M., Moore, R., Kipman, A., and Blake, A. (2011). Real-Time Human Pose Recognition in Parts from Single Depth Images. In *Conference on Computer Vision and Pattern Recognition*, volume 2, pages 1297–1304.
- Tomasi, C. (1998). Bilateral Filtering for Gray and Color Images. In *International Conference on Computer Vision*, pages 839–846.
- Yang, Q., Yang, R., Davis, J., and Nister, D. (2007). Spatial-Depth Super Resolution for Range Images. In *Conference on Computer Vision and Pattern Recognition*, pages 1–8.